

# $\Lambda NN$ and $\Sigma NN$ systems at threshold: II. The effect of $D$ waves

H. Garcilazo<sup>(1)</sup>, A. Valcarce<sup>(2)</sup>, and T. Fernández-Caramés<sup>(3)</sup>

- (1) *Escuela Superior de Física y Matemáticas, Instituto Politécnico Nacional, Edificio 9, 07738 México D.F., Mexico*  
(2) *Departamento de Física Fundamental, Universidad de Salamanca, E-37008 Salamanca, Spain*  
(3) *Departamento de Física Teórica e IFIC, Universidad de Valencia - CSIC, E-46100 Burjassot, Valencia, Spain*

## Abstract

Using the two-body interactions obtained from a chiral constituent quark model we study all  $\Lambda NN$  and  $\Sigma NN$  states with  $I = 0, 1, 2$  and  $J = 1/2, 3/2$  at threshold, taking into account all three-body configurations with  $S$  and  $D$  wave components. We constrain further the limits for the  $\Lambda N$  spin-triplet scattering length  $a_{1/2,1}$ . Using the hypertriton binding energy we find a narrow interval for the possible values of the  $\Lambda N$  spin-singlet scattering length  $a_{1/2,0}$ . We found that the  $\Sigma NN$  system has a quasibound state in the  $(I, J) = (1, 1/2)$  channel very near threshold with a width of about 2.1 MeV.

## I. INTRODUCTION

The chiral constituent quark model has been very successful in the simultaneous description of the baryon-baryon interaction and the baryon spectrum as well as in the study of the two- and three-baryon bound-state problem for the nonstrange sector [1]. A simple generalization of this model to the strange sector has been applied to study the meson and baryon spectra [2] and the  $\Sigma NN$  bound-state problem [3]. Recently, a more elaborated description of the model was developed in Ref. [4], where the  $\Lambda NN$  system was also studied.

In Ref. [4] we studied the  $\Lambda NN$  and  $\Sigma NN$  systems at threshold by solving the Faddeev equations of the coupled  $\Lambda NN - \Sigma NN$  system in the case of pure  $S$  wave configurations for the channels  $(I, J)$  with  $I = 0, 1, 2$  and  $J = 1/2, 3/2$ . However, since the hyperon-nucleon and nucleon-nucleon interactions contain sizeable tensor terms there is a coupling between the  $\ell = 0$  and  $\ell = 2$  baryon-baryon channels and between the hyperon-nucleon-nucleon channels with  $\ell = 0$  and  $\lambda = 0$  to the channels with  $\ell = 2$  and  $\lambda = 2$ . The importance of the tensor force at the two-body level manifests itself dramatically in the case of the  $\Sigma^- p \rightarrow \Lambda n$  process which is dominated by the  $\Sigma N(\ell = 0) \rightarrow \Lambda N(\ell = 2)$  transition such that if one includes only the  $\Sigma N(\ell = 0) \rightarrow \Lambda N(\ell = 0)$  transition it is practically impossible to describe the cross section [3] (this problem was first observed in Ref. [5]). Thus, one expects that also at the three-body level the effect of the  $D$  waves will be important.

In Refs. [3,4] we considered all configurations where the baryon-baryon subsystems are in an  $S$  wave and the third particle is also in an  $S$  wave with respect to the pair. However, to construct the two-body  $t$ -matrices that serve as input of the Faddeev equations we considered the full interaction including the contribution of the  $D$  waves and of course the coupling between the  $\Sigma N$  and  $\Lambda N$  subsystems (which is known as the truncated  $t$ -matrix approximation [6]). In Ref. [4] we found that our model with only  $S$  waves is able to predict correctly the binding energy of the hypertriton, which is a bound state in the channel  $(I, J) = (0, 1/2)$ . We also found that the channel  $(I, J) = (0, 3/2)$  will develop a bound state if the triplet  $\Lambda N$  scattering length  $a_{1/2,1}$  is larger than 1.68 fm. In the case of the  $\Sigma NN$  system the channel  $(I, J) = (1, 1/2)$  develops a quasibound state in some cases while the channel  $(I, J) = (0, 1/2)$  is also attractive but unbound.

In this work, we will further pursue the study of the  $\Lambda NN - \Sigma NN$  system at threshold when the three-body  $D$  wave components are considered. We will analyze their effects comparing our results with those obtained when using only three-body  $S$  wave contributions. The structure of the paper is the following. In the next section we will resume the basic aspects of the two-body interactions and we will present the generalization of the Faddeev equations of Ref. [4] for arbitrary orbital angular momenta. In section III we present our results as compared to those of Ref. [4] to discuss the effect of the three-body  $D$  waves. Finally, in section IV we summarize our main conclusions.

## II. FORMALISM

### A. The two-body interactions

The baryon-baryon interactions involved in the study of the coupled  $\Sigma NN - \Lambda NN$  system are obtained from the chiral constituent quark model [1,2]. In this model baryons are described as clusters of three interacting massive (constituent) quarks, the mass coming from the spontaneous breaking of chiral symmetry. The first ingredient of the quark-quark interaction is a confining potential ( $CON$ ). Perturbative aspects of QCD are taken into account by means of a one-gluon potential ( $OGE$ ). Spontaneous breaking of chiral symmetry gives rise to boson exchanges between quarks. In particular, there appear pseudoscalar boson exchanges and their corresponding scalar partners [4]. Thus, the quark-quark interaction will read:

$$V_{qq}(\vec{r}_{ij}) = V_{CON}(\vec{r}_{ij}) + V_{OGE}(\vec{r}_{ij}) + V_{\chi}(\vec{r}_{ij}) + V_S(\vec{r}_{ij}) , \quad (1)$$

where the  $i$  and  $j$  indices are associated with  $i$  and  $j$  quarks respectively, and  $\vec{r}_{ij}$  stands for the interquark distance.  $V_{\chi}$  denotes the pseudoscalar meson-exchange interaction discussed in Ref. [3], and  $V_S$  stands for the scalar meson-exchange potential described in Ref. [4]. Explicit expressions of all the interacting potentials and a more detailed discussion of the model can be found in Refs. [2,4]. In order to derive the local  $B_1 B_2 \rightarrow B_3 B_4$  potentials from the basic  $qq$  interaction defined above we use a Born-Oppenheimer approximation. Explicitly, the potential is calculated as follows,

$$V_{B_1 B_2(LST) \rightarrow B_3 B_4(L'S'T)}(R) = \xi_{LST}^{L'S'T}(R) - \xi_{LST}^{L'S'T}(\infty) , \quad (2)$$

where

$$\xi_{LST}^{L'S'T}(R) = \frac{\langle \Psi_{B_3 B_4}^{L'S'T}(\vec{R}) | \sum_{i < j=1}^6 V_{qq}(\vec{r}_{ij}) | \Psi_{B_1 B_2}^{LST}(\vec{R}) \rangle}{\sqrt{\langle \Psi_{B_3 B_4}^{L'S'T}(\vec{R}) | \Psi_{B_3 B_4}^{L'S'T}(\vec{R}) \rangle} \sqrt{\langle \Psi_{B_1 B_2}^{LST}(\vec{R}) | \Psi_{B_1 B_2}^{LST}(\vec{R}) \rangle}} . \quad (3)$$

In the last expression the quark coordinates are integrated out keeping  $R$  fixed, the resulting interaction being a function of the  $B_i - B_j$  relative distance. The wave function  $\Psi_{B_i B_j}^{LST}(\vec{R})$  for the two-baryon system is discussed in detail in Ref. [1].

### B. Faddeev equations at threshold

Our method [3] to transform the Faddeev equations from being integral equations in two continuous variables into integral equations in just one continuous variable is based in the expansion of the two-body  $t$ -matrices

$$t_i(p_i, p'_i; e) = \sum_{nr} P_n(x_i) \tau_i^{nr}(e) P_r(x'_i), \quad (4)$$

where  $P_n$  and  $P_r$  are Legendre polynomials,

$$x_i = \frac{p_i - b}{p_i + b}, \quad (5)$$

$$x'_i = \frac{p'_i - b}{p'_i + b}, \quad (6)$$

and  $p_i$  and  $p'_i$  are the initial and final relative momenta of the pair  $jk$  while  $b$  is a scale parameter on which the results do not depend.

In Ref. [4] we wrote down the integral equations for  $\beta d$  scattering at threshold with  $\beta = \Sigma$  or  $\Lambda$  including the full coupling between  $\Lambda NN$  and  $\Sigma NN$  states for the case of pure  $S$  wave configurations assuming that particle 1 is the hyperon and particles 2 and 3 are the two nucleons. In order to include arbitrary orbital angular momentum configurations we consider the total angular momentum and total isospin  $J$  and  $I$  while  $\sigma_1$  ( $\tau_1$ ) and  $\sigma_3$  ( $\tau_3$ ) stand for the spin (isospin) of the hyperon and the nucleon respectively. In addition,  $\ell_i$ ,  $s_i$ ,  $j_i$ ,  $i_i$ ,  $\lambda_i$ , and  $J_i$  are the orbital angular momentum, spin, total angular momentum, and isospin of the pair  $jk$  while  $\lambda_i$  is the orbital angular momentum between particle  $i$  and the pair  $jk$  and  $J_i$  is the result of coupling  $\lambda_i$  and  $\sigma_i$ . If in Eqs. (10)–(14) of Ref. [4] we make the replacements

$$\{ns_2i_2\} \rightarrow \{n\ell_2s_2j_2i_2\lambda_2J_2\} \equiv \gamma_2, \quad (7)$$

$$\{ms_3i_3\} \rightarrow \{m\ell_3s_3j_3i_3\lambda_3J_3\} \equiv \gamma_3, \quad (8)$$

$$\{rs_1i_1\} \rightarrow \{r\ell_1s_1j_1i_1\lambda_1J_1\} \equiv \gamma_1, \quad (9)$$

the three-body equations become

$$\begin{aligned} T_{2;JI;\beta}^{\gamma_2}(q_2) &= B_{2;JI;\beta}^{\gamma_2}(q_2) + \sum_{\gamma_3} \int_0^\infty dq_3 \left[ (-1)^{1+\ell_2+\sigma_1+\sigma_3-s_2+\tau_1+\tau_3-i_2} A_{23;JI}^{\gamma_2\gamma_3}(q_2, q_3; E) \right. \\ &\quad \left. + 2 \sum_{\gamma_1} \int_0^\infty dq_1 A_{31;JI}^{\gamma_2\gamma_1}(q_2, q_1; E) A_{13;JI}^{\gamma_1\gamma_3}(q_1, q_3; E) \right] T_{2;JI;\beta}^{\gamma_3}(q_3), \end{aligned} \quad (10)$$

where  $T_{2;SI;\beta}^{\gamma_2}(q_2)$  is a two-component vector

$$T_{2;JI;\beta}^{\gamma_2}(q_2) = \begin{pmatrix} T_{2;JI;\Sigma\beta}^{\gamma_2}(q_2) \\ T_{2;JI;\Lambda\beta}^{\gamma_2}(q_2) \end{pmatrix}, \quad (11)$$

while the kernel of Eq. (10) is a  $2 \times 2$  matrix defined by

$$A_{23;JI}^{\gamma_2\gamma_3}(q_2, q_3; E) = \begin{pmatrix} A_{23;JI;\Sigma\Sigma}^{\gamma_2\gamma_3}(q_2, q_3; E) & A_{23;JI;\Sigma\Lambda}^{\gamma_2\gamma_3}(q_2, q_3; E) \\ A_{23;JI;\Lambda\Sigma}^{\gamma_2\gamma_3}(q_2, q_3; E) & A_{23;JI;\Lambda\Lambda}^{\gamma_2\gamma_3}(q_2, q_3; E) \end{pmatrix}, \quad (12)$$

$$A_{31;JI}^{\gamma_2\gamma_1}(q_2, q_1; E) = \begin{pmatrix} A_{31;JI;\Sigma N(\Sigma)}^{\gamma_2\gamma_1}(q_2, q_1; E) & A_{31;JI;\Sigma N(\Lambda)}^{\gamma_2\gamma_1}(q_2, q_1; E) \\ A_{31;JI;\Lambda N(\Sigma)}^{\gamma_2\gamma_1}(q_2, q_1; E) & A_{31;JI;\Lambda N(\Lambda)}^{\gamma_2\gamma_1}(q_2, q_1; E) \end{pmatrix}, \quad (13)$$

$$A_{13;JI}^{\gamma_1\gamma_3}(q_1, q_3; E) = \begin{pmatrix} A_{13;JI;N\Sigma}^{\gamma_1\gamma_3}(q_1, q_3; E) & 0 \\ 0 & A_{13;JI;N\Lambda}^{\gamma_1\gamma_3}(q_1, q_3; E) \end{pmatrix}, \quad (14)$$

where

$$A_{23;JI;\alpha\beta}^{\gamma_2\gamma_3}(q_2, q_3; E) = \sum_{\ell'_2 r} \tau_{2;\ell_2\ell'_2 s_2 j_2 i_2; \alpha\beta}^{nr} (E - q_2^2/2\nu_2) \frac{q_3^2}{2} \\ \times \int_{-1}^1 d\cos\theta \frac{P_r(x'_2) D_{23;JI;\beta}^{\rho'_2\rho_3}(q_2, q_3, \cos\theta) P_m(x_3)}{E + \Delta E \delta_{\beta\Lambda} - p_3^2/2\mu_3 - q_3^2/2\nu_3 + i\epsilon}; \quad \alpha, \beta = \Sigma, \Lambda, \quad (15)$$

$$A_{31;JI;\alpha N(\beta)}^{\gamma_2\gamma_1}(q_2, q_1; E) = \sum_{\ell'_2 r} \tau_{3;\ell_2\ell'_2 s_2 j_2 i_2; \alpha\beta}^{nr} (E - q_2^2/2\nu_2) \frac{q_1^2}{2} \\ \times \int_{-1}^1 d\cos\theta \frac{P_r(x'_3) D_{31;JI;\beta}^{\rho'_2\rho_1}(q_2, q_1, \cos\theta) P_m(x_1)}{E + \Delta E \delta_{\beta\Lambda} - p_1^2/2\mu_1 - q_1^2/2\nu_1 + i\epsilon}; \quad \alpha, \beta = \Sigma, \Lambda, \quad (16)$$

$$A_{13;JI;N\beta}^{\gamma_1\gamma_3}(q_1, q_3; E) = \sum_{\ell'_1 r} \tau_{1;\ell_1\ell'_1 s_1 j_1 i_1; NN}^{nr} (E + \Delta E \delta_{\beta\Lambda} - q_1^2/2\nu_1) \frac{q_3^2}{2} \\ \times \int_{-1}^1 d\cos\theta \frac{P_r(x'_1) D_{13;JI;\beta}^{\rho_1'\rho_3}(q_1, q_3, \cos\theta) P_m(x_3)}{E + \Delta E \delta_{\beta\Lambda} - p_3^2/2\mu_3 - q_3^2/2\nu_3 + i\epsilon}; \quad \beta = \Sigma, \Lambda, \quad (17)$$

where

$$\rho_i \equiv \{\ell_i s_i j_i i_i \lambda_i J_i\}, \quad (18)$$

$$\rho'_i \equiv \{\ell'_i s_i j_i i_i \lambda_i J_i\}, \quad (19)$$

and  $\eta_i$  and  $\nu_i$  are the usual reduced masses

$$\eta_i = \frac{m_j m_k}{m_j + m_k}, \\ \nu_i = \frac{m_i(m_j + m_k)}{m_i + m_j + m_k}. \quad (20)$$

In Eqs. (15)–(20) the isospin and mass of particle 1 (the hyperon) is determined by the subindex  $\beta$ . The subindex  $\alpha N(\beta)$  in Eq. (16) indicates a transition  $\alpha N \rightarrow \beta N$  with a nucleon as spectator followed by a  $NN \rightarrow NN$  transition with  $\beta$  as spectator. The angular momentum functions  $D_{ij;JI;\beta}^{\rho_i\rho_j}(q_i, q_j, \cos\theta)$  are given by

$$D_{ij;JI;\beta}^{\rho_i\rho_j}(q_i, q_j, \cos\theta) = (-)^{i_j+\tau_j-I} \sqrt{(2i_i+1)(2i_j+1)} W(\tau_j \tau_k I \tau_i; i_i i_j) \\ \times \sqrt{(2j_i+1)(2j_j+1)(2J_i+1)(2J_j+1)} \\ \times \sum_{LS} (2L+1)(2S+1) \begin{Bmatrix} \ell_i & \lambda_i & L \\ s_i & \sigma_i & S \\ j_i & J_i & J \end{Bmatrix} \begin{Bmatrix} \ell_j & \lambda_j & L \\ s_j & \sigma_j & S \\ j_j & J_j & J \end{Bmatrix}$$

$$\begin{aligned}
& \times (-)^{s_j + \sigma_j - S} \sqrt{(2s_i + 1)(2s_j + 1)} W(\sigma_j \sigma_k S \sigma_i; s_i s_j) \\
& \times \frac{1}{2L + 1} \sum_{M m_i m_j} C_{m_i, M - m_i, M}^{\ell_i \lambda_i L} C_{m_j, M - m_j, M}^{\ell_j \lambda_j L} \Gamma_{\ell_i m_i} \Gamma_{\lambda_i M - m_i} \\
& \times \Gamma_{\ell_j m_j} \Gamma_{\lambda_j M - m_j} \cos(-M\theta - m_i \theta_i + m_j \theta_j),
\end{aligned} \tag{21}$$

where  $W$  is the Racah coefficient and  $\Gamma_{\ell m} = 0$  if  $\ell - m$  is odd while

$$\Gamma_{\ell m} = \frac{(-)^{(\ell+m)/2} \sqrt{(2\ell + 1)(\ell + m)!(\ell - m)!}}{2^\ell ((\ell + m)/2)! ((\ell - m)/2)!}, \tag{22}$$

if  $\ell - m$  is even. The angles  $\theta$ ,  $\theta_i$ , and  $\theta_j$  are given by

$$\cos \theta = \frac{\vec{q}_i \cdot \vec{q}_j}{q_i q_j}, \tag{23}$$

$$\cos \theta_i = \frac{\vec{q}_i \cdot \vec{p}_i}{q_i p_i}, \tag{24}$$

$$\cos \theta_j = \frac{\vec{q}_j \cdot \vec{p}_j}{q_j p_j}, \tag{25}$$

with

$$\begin{aligned}
\vec{p}_i &= -\vec{q}_j - \frac{\eta_i}{m_k} \vec{q}_i, \\
\vec{p}_j &= \vec{q}_i + \frac{\eta_j}{m_k} \vec{q}_j.
\end{aligned} \tag{26}$$

$\tau_{i; \ell_i \ell'_i s_i j_i i_i; \alpha \beta}^{nr}(e)$  are the coefficients of the expansion in terms of Legendre polynomials of the hyperon-nucleon  $t$ -matrix  $t_{i; \ell_i \ell'_i s_i j_i i_i; \alpha \beta}(p_i, p'_i; e)$  for the transition  $\alpha N \rightarrow \beta N$ , i.e.,

$$\tau_{i; \ell_i \ell'_i s_i j_i i_i; \alpha \beta}^{nr}(e) = \frac{2n + 1}{2} \frac{2r + 1}{2} \int_{-1}^1 dx_i \int_{-1}^1 dx'_i P_n(x_i) t_{i; \ell_i \ell'_i s_i j_i i_i; \alpha \beta}(p_i, p'_i; e) P_r(x'_i). \tag{27}$$

The energy shift,  $\Delta E$ , is chosen such that at the  $\beta d$  threshold the momentum of the  $\alpha d$  system has the correct value, i.e.,

$$\Delta E = \frac{[(m_\beta + m_d)^2 - (m_\alpha + m_d)^2][(m_\beta + m_d)^2 - (m_\alpha - m_d)^2]}{8\mu_{\alpha d}(m_\beta + m_d)^2}, \tag{28}$$

where  $\mu_{\alpha d}$  is the  $\alpha d$  reduced mass.

The inhomogeneous term of Eq. (10),  $B_{2; JI; \beta}^{\gamma_2}(q_2)$  is a two-component vector

$$B_{2; JI; \beta}^{\gamma_2}(q_2) = \begin{pmatrix} B_{2; JI; \Sigma \beta}^{\gamma_2}(q_2) \\ B_{2; JI; \Lambda \beta}^{\gamma_2}(q_2) \end{pmatrix}, \tag{29}$$

where

$$B_{2;JI;\alpha\beta}^{\gamma_2}(q_2) = \sum_{\ell'_2 r \rho_{10}} \tau_{2;\ell_2 \ell'_2 s_2 j_2 i_2; \alpha\beta}^{nr} (E_\beta^{th} - q_2^2/2\nu_2) \times P_r(x'_2) D_{31;JI;\beta}^{\rho'_2 \rho_{10}}(q_2, 0, 0) \phi_{d;l_1}(q_2), \quad (30)$$

and

$$\rho_{10} \equiv \{\ell_1, s_1 = 1, j_1 = 1, i_1 = 0, \lambda_1 = 0, J_1\}, \quad (31)$$

which corresponds to a hyperon-deuteron initial state,  $\phi_{d;\ell_1}(q_2)$  is the deuteron wave function with orbital angular momentum  $\ell_1$ ,  $E_\beta^{th}$  is the energy of the  $\beta d$  threshold,  $P_r(x'_2)$  is a Legendre polynomial of order  $r$ , and

$$x'_2 = \frac{\frac{\eta_2}{m_3} q_2 - b}{\frac{\eta_2}{m_3} q_2 + b}. \quad (32)$$

Finally, after solving the inhomogeneous set of equations (10), the  $\beta d$  scattering length is given by

$$A_{\beta d} = -\pi \mu_{\beta d} T_{\beta\beta}, \quad (33)$$

with

$$T_{\beta\beta} = 2 \sum_{n \rho_{10} \rho_2} \int_0^\infty q_2^2 dq_2 \phi_{d;\ell_1}(q_2) P_n(x'_2) D_{13;JI;\beta}^{\rho_{10} \rho_2}(0, q_2, 0) T_{2;JI;\beta\beta}^{\gamma_2}(q_2). \quad (34)$$

In the case of the  $\Sigma NN$  system, even for energies below the  $\Sigma d$  threshold, one encounters the three-body singularities of the  $\Lambda NN$  system so that to solve the integral equations (10) one has to use the contour rotation method where the momenta are rotated into the complex plane  $q_i \rightarrow q_i e^{-i\phi}$  since as pointed out in Ref. [3] the results do not depend on the contour rotation angle  $\phi$ .

We give in Table I the two-body channels that contribute in the case of the six three-body channels  $(I, J)$  with  $I = 0, 1, 2$  and  $J = 1/2, 3/2$ . For the parameter  $b$  in Eqs. (5) and (6) we found that  $b = 3 \text{ fm}^{-1}$  leads to very stable results while for the expansion (4) we took twelve Legendre polynomials, i.e.,  $0 \leq n \leq 11$ .

### III. RESULTS

In Ref. [4] we constructed different families of interacting potentials, by introducing small variations of the mass of the effective scalar exchange potentials, that allow us to study the dependence of the results on the strength of the spin-singlet and spin-triplet hyperon-nucleon interactions. These potentials are characterized by the  $\Lambda N$  scattering lengths  $a_{i,s}$  and they reproduce the cross sections near threshold of the five hyperon-nucleon processes for which data are available (see Ref. [4]).

## A. The $\Lambda NN$ system

The channels  $(I, J) = (0, 1/2)$  and  $(0, 3/2)$  are the most attractive ones of the  $\Lambda NN$  system. In particular, the channel  $(0, 1/2)$  has the only bound state of this system, the hypertriton. We give in Table II the results of the models constructed in Ref. [4] for the two  $\Lambda d$  scattering lengths and the hypertriton binding energy. We compare with the results, in parentheses, obtained in Ref. [4] including only the three-body  $S$  wave configurations. As a consequence of considering the  $D$  waves, the hypertriton binding energy increases by about 50–60 keV [7], while the  $A_{0,1/2}$  scattering length decreases by about 3–5 fm. The largest changes occur in the  $A_{0,3/2}$  scattering length where both positive and negative values appeared which means, in the case of the negative values, that a bound state is generated in the  $(I, J) = (0, 3/2)$  channel. Since this channel depends mainly on the spin-triplet hyperon-nucleon interaction and experimentally there is no evidence whatsoever for the existence of a  $(I, J) = (0, 3/2)$  bound state one can use the results of this channel to set limits on the value of the hyperon-nucleon spin-triplet scattering length  $a_{1/2,1}$ . We plot in Fig. 1 the inverse of the two  $\Lambda d$  scattering lengths as a function of the spin-triplet  $\Lambda N$  scattering length  $a_{1/2,1}$ . As one can see, increasing  $a_{1/2,1}$  one increases the amount of attraction that is present in the system since the three-body channel  $(I, J) = (0, 3/2)$  becomes bound if  $a_{1/2,1} > 1.58$  fm. Moreover, we found in Ref. [4] that the fit of the hyperon-nucleon cross sections is worsened for those cases where the spin-triplet  $\Lambda N$  scattering length is smaller than 1.41 fm, so that we conclude that  $1.41 \leq a_{1/2,1} \leq 1.58$  fm. This range of values is narrower than the one found in Ref. [4].

In order to show the dependence of these results on the spin-singlet  $\Lambda N$  scattering length  $a_{1/2,0}$  we have also plotted in Fig. 1 the results of the last three rows of Table II where  $a_{1/2,1} = 1.65$  fm and  $a_{1/2,0} = 2.31, 2.55$ , and  $2.74$  fm (they are denoted by *diamonds*). As one can see,  $1/A_{0,3/2}$  almost does not change although there is a large sensitivity in  $1/A_{0,1/2}$ . In order to try to set some limits to the hyperon-nucleon spin-singlet scattering length, we have calculated in Table III the hypertriton binding energy using for the hyperon-nucleon spin-triplet scattering length the allowed values  $1.41 \leq a_{1/2,1} \leq 1.58$  fm and using for the spin-singlet scattering length  $2.33 \leq a_{1/2,0} \leq 2.48$  fm which leads to results for the hypertriton binding energy within the experimental error bars  $B_{0,1/2} = 0.13 \pm 0.05$  MeV.

With regard to the isospin 1 channels  $(I, J) = (1, 1/2)$  and  $(1, 3/2)$ , we show in Fig. 2 the Fredholm determinant of these channels for energies below the  $\Lambda NN$  threshold where one sees that the  $(1, 1/2)$  channel is attractive but not enough to produce a bound state while the  $(1, 3/2)$  channel is repulsive. These results are very similar to the ones found in Ref. [4].

## B. The $\Sigma NN$ system

We show in Table IV the  $\Sigma d$  scattering lengths  $A'_{1,3/2}$  and  $A'_{1,1/2}$ . The  $\Sigma d$  scattering lengths are complex since the inelastic  $\Lambda NN$  channels are always open. The scattering length  $A'_{1,3/2}$  depends mainly on the spin-triplet hyperon-nucleon channels and both its real and imaginary parts increase when the spin-triplet hyperon-nucleon scattering length increases. The effect of the three-body  $D$  waves is to lower the real part by about 20 % and the imaginary part by about 10 %. The scattering length  $A'_{1,1/2}$  shows large variations



between the results with and without three-body  $D$  waves but this is due, as we will see next, to the fact that there is a pole very near threshold, a situation quite similar to that of the  $A_{0,3/2}$   $\Lambda d$  scattering length discussed in the previous subsection.

We plot in Fig. 3 the real and imaginary parts of the  $\Sigma d$  scattering length  $A'_{1,1/2}$  as functions of the spin-triplet  $\Lambda N$  scattering length  $a_{1/2,1}$ , since by increasing  $a_{1/2,1}$  one is increasing the amount of attraction that is present in the three-body channel. As one can see,  $\text{Re}(A'_{1,1/2})$  changes sign going from positive to negative while at the same time  $\text{Im}(A'_{1,1/2})$  has a maximum. These two features are the typical ones that signal that the channel has a quasibound state [8]. Since in the case of the  $\Sigma NN$  system we are using the contour rotation method which opens large portions of the second Riemann sheet we can search for the position of this pole in the complex plane which is given in the last column of Table IV. As one can see the position of the pole changes very little with the model used to calculate it and it lies at around  $2.8 - i 2.1$  MeV. The diagram that gives the most important contribution to the width of this state is the one drawn in Fig. 4, since the process  $\Sigma N \rightarrow \Lambda N$  is dominated by the transition  ${}^3S_1 \rightarrow {}^3D_1$ . For example, at  $p_{\text{LAB}}^\Sigma = 40$  MeV/c, the on-shell transition potential  $V_{\Sigma\Lambda}({}^3S_1 \rightarrow {}^3D_1) = 4.542 \cdot 10^{-2}$  fm<sup>2</sup>, while  $V_{\Sigma\Lambda}({}^3S_1 \rightarrow {}^3S_1) = -1.008 \cdot 10^{-2}$  fm<sup>2</sup>, a factor four smaller. The corresponding on-shell transition amplitudes are  $t_{\Sigma\Lambda}({}^3S_1 \rightarrow {}^3D_1) = 8.520 \cdot 10^{-2} + i 5.507 \cdot 10^{-2}$  fm<sup>2</sup>, and  $t_{\Sigma\Lambda}({}^3S_1 \rightarrow {}^3S_1) = -1.061 \cdot 10^{-2} - i 8.961 \cdot 10^{-3}$  fm<sup>2</sup>, roughly a factor eight smaller.

We show in Fig. 5 the real part of the Fredholm determinant of the six  $(I, J)$   $\Sigma NN$  channels that are possible for energies below the  $\Sigma d$  threshold. The imaginary part of the Fredholm determinant is small and uninteresting. As one can see the channel  $(1, 1/2)$  is the most attractive one since the Fredholm determinant is close to zero at the  $\Sigma d$  threshold, which as mentioned before, indicates the presence of a quasibound state. The next channel, in what to amount of attraction is concerned, is the  $(I, J) = (0, 1/2)$ . The ordering of the two attractive  $\Sigma NN$   $J = 1/2$  channels can be easily understood by looking at Table III of Ref. [4]. All the attractive two-body channels in the  $NN$ ,  $\Lambda N$ , and  $\Sigma N$  subsystems contribute to the  $(I, J) = (1, 1/2)$   $\Sigma NN$  state (the  $\Sigma N$  channels  ${}^3S_1(I = 1/2)$  and  ${}^1S_0(I = 3/2)$  and the  ${}^3S_1(I = 0)$   $NN$  channel), while the  $(I, J) = (0, 1/2)$  state does not present contribution from two of them, the  ${}^1S_0(I = 3/2)$   $\Sigma N$  and specially the  ${}^3S_1(I = 0)$   $NN$  deuteron channel.

#### IV. SUMMARY

We have solved the Faddeev equations for the  $\Lambda NN$  and  $\Sigma NN$  systems using the hyperon-nucleon and nucleon-nucleon interactions derived from a chiral constituent quark model with full inclusion of the  $\Lambda \leftrightarrow \Sigma$  conversion and taking into account all three-body configurations with  $S$  and  $D$  wave components.

In the case of the  $\Lambda NN$  system the inclusion of the three-body  $D$  wave components increases the attraction, reducing the upper limit of the  $a_{1/2,1}$   $\Lambda N$  scattering length if the  $(I, J) = (0, 3/2)$   $\Lambda NN$  bound state does not exist. This state shows a somewhat larger sensitivity than the hypertriton to the three-body  $D$  waves. Our calculation including the three-body  $D$  wave configurations of all relevant observables of two- and three-baryon systems with strangeness  $-1$ , permits to constrain the  $\Lambda N$  scattering lengths to:  $1.41 \leq a_{1/2,1} \leq 1.58$  fm and  $2.33 \leq a_{1/2,0} \leq 2.48$  fm.

In the case of the  $\Sigma NN$  system there exists a narrow quasibound state near threshold in the  $(I, J) = (1, 1/2)$  channel. The width of this state, of the order of 2.1 MeV, comes mainly from the coupling to the  $\Lambda NN$  system in a  $D$  wave three-body channel.

The actual interest in two- and three-baryon systems with strangeness  $-1$  [9] makes worthwhile to pursue the experimental search of narrow peaks near threshold related with the predictions of our model based on the description of almost all known observables of the two- and three-baryons with strangeness  $-1$ .

## ACKNOWLEDGMENTS

This work has been partially funded by Ministerio de Educación y Ciencia under Contract No. FPA2004-05616 and by COFAA-IPN (México).

## REFERENCES

- [1] A. Valcarce, H. Garcilazo, F. Fernández, and P. González, Rep. Prog. Phys. **68**, 965 (2005).
- [2] A. Valcarce, H. Garcilazo, and J. Vijande, Phys. Rev. C **72**, 025206 (2005). J. Vijande, F. Fernández, and A. Valcarce, J. Phys. G **31**, 481 (2005).
- [3] T. Fernández-Caramés, A. Valcarce, H. Garcilazo, and P. González, Phys. Rev. C **73**, 034004 (2006).
- [4] H. Garcilazo, T. Fernández-Caramés, and A. Valcarce, Phys. Rev. C **75**, 034002 (2007).
- [5] U. Straub, Z. Zhang, K. Bräuer, A. Faessler, S.B. Khadkikar, Nucl. Phys. A **483**, 686 (1988).
- [6] G.H. Berthold, H. Zankel, L. Mathelitsch, and H. Garcilazo, Il Nuovo Cimento A **93**, 89 (1986).
- [7] Y. Fujiwara, K. Miyagawa, M. Kohno, and Y. Suzuki, Phys. Rev. C **70**, 024001 (2004).
- [8] A. Deloff, Phys. Rev. C **61**, 024004 (2000).
- [9] FINUDA Collaboration, M. Palomba, AIP Conf. Proc. **842**, 421 (2006). KEK-PS E471/E549 Collaboration, M. Sato, AIP Conf. Proc. **842**, 480 (2006).

# TABLES

TABLE I. Two-body  $\Sigma N$  channels with a nucleon as spectator  $(\ell_{\Sigma} s_{\Sigma} j_{\Sigma} i_{\Sigma} \lambda_{\Sigma} J_{\Sigma})_N$ , two-body  $\Lambda N$  channels with a nucleon as spectator  $(\ell_{\Lambda} s_{\Lambda} j_{\Lambda} i_{\Lambda} \lambda_{\Lambda} J_{\Lambda})_N$ , two-body  $NN$  channels with a  $\Sigma$  as spectator  $(\ell_{N} s_{N} j_{N} i_{N} \lambda_{N} J_{N})_{\Sigma}$ , and two-body  $NN$  channels with a  $\Lambda$  as spectator  $(\ell_{N} s_{N} j_{N} i_{N} \lambda_{N} J_{N})_{\Lambda}$  that contribute to a given  $\Sigma NN - \Lambda NN$  state with total isospin  $I$  and total angular momentum  $J$ .

$I$	$J$	$(\ell_{\Sigma} s_{\Sigma} j_{\Sigma} i_{\Sigma} \lambda_{\Sigma} J_{\Sigma})_N$	$(\ell_{\Lambda} s_{\Lambda} j_{\Lambda} i_{\Lambda} \lambda_{\Lambda} J_{\Lambda})_N$	$(\ell_{N} s_{N} j_{N} i_{N} \lambda_{N} J_{N})_{\Sigma}$	$(\ell_{N} s_{N} j_{N} i_{N} \lambda_{N} J_{N})_{\Lambda}$
0	$\frac{1}{2}$	$(000\frac{1}{2}0\frac{1}{2}), (011\frac{1}{2}0\frac{1}{2}),$ $(211\frac{1}{2}0\frac{1}{2}), (011\frac{1}{2}2\frac{3}{2}),$ $(211\frac{1}{2}2\frac{3}{2})$	$(000\frac{1}{2}0\frac{1}{2}), (011\frac{1}{2}0\frac{1}{2}),$ $(211\frac{1}{2}0\frac{1}{2}), (011\frac{1}{2}2\frac{3}{2}),$ $(211\frac{1}{2}2\frac{3}{2})$	$(00010\frac{1}{2})$	$(01100\frac{1}{2}), (21100\frac{1}{2}),$ $(01102\frac{3}{2}), (21102\frac{3}{2})$
1	$\frac{1}{2}$	$(000\frac{1}{2}0\frac{1}{2}), (011\frac{1}{2}0\frac{1}{2}),$ $(211\frac{1}{2}0\frac{1}{2}), (011\frac{1}{2}2\frac{3}{2}),$ $(211\frac{1}{2}2\frac{3}{2}), (000\frac{3}{2}0\frac{1}{2}),$ $(011\frac{3}{2}0\frac{1}{2}), (211\frac{3}{2}0\frac{1}{2}),$ $(011\frac{3}{2}2\frac{3}{2}), (211\frac{3}{2}2\frac{3}{2})$	$(000\frac{1}{2}0\frac{1}{2}), (011\frac{1}{2}0\frac{1}{2}),$ $(211\frac{1}{2}0\frac{1}{2}), (011\frac{1}{2}2\frac{3}{2}),$ $(211\frac{1}{2}2\frac{3}{2})$	$(00010\frac{1}{2}), (01100\frac{1}{2}),$ $(21100\frac{1}{2}), (01102\frac{3}{2}),$ $(21102\frac{3}{2})$	$(00010\frac{1}{2})$
2	$\frac{1}{2}$	$(000\frac{3}{2}0\frac{1}{2}), (011\frac{3}{2}0\frac{1}{2}),$ $(211\frac{3}{2}0\frac{1}{2}), (011\frac{3}{2}2\frac{3}{2}),$ $(211\frac{3}{2}2\frac{3}{2})$		$(00010\frac{1}{2})$	
0	$\frac{3}{2}$	$(000\frac{1}{2}2\frac{3}{2}), (011\frac{1}{2}0\frac{1}{2}),$ $(211\frac{1}{2}0\frac{1}{2}), (011\frac{1}{2}2\frac{3}{2}),$ $(011\frac{1}{2}2\frac{5}{2}), (211\frac{1}{2}2\frac{3}{2}),$ $(211\frac{1}{2}2\frac{5}{2})$	$(000\frac{1}{2}2\frac{3}{2}), (011\frac{1}{2}0\frac{1}{2}),$ $(211\frac{1}{2}0\frac{1}{2}), (011\frac{1}{2}2\frac{3}{2}),$ $(011\frac{1}{2}2\frac{5}{2}), (211\frac{1}{2}2\frac{3}{2}),$ $(211\frac{1}{2}2\frac{5}{2})$	$(00012\frac{3}{2})$	$(01100\frac{1}{2}), (21100\frac{1}{2}),$ $(01102\frac{3}{2}), (01102\frac{5}{2}),$ $(21102\frac{3}{2}), (21102\frac{5}{2})$
1	$\frac{3}{2}$	$(000\frac{1}{2}2\frac{3}{2}), (011\frac{1}{2}0\frac{1}{2}),$ $(211\frac{1}{2}0\frac{1}{2}), (011\frac{1}{2}2\frac{3}{2}),$ $(011\frac{1}{2}2\frac{5}{2}), (211\frac{1}{2}2\frac{3}{2}),$ $(211\frac{1}{2}2\frac{5}{2}), (000\frac{3}{2}2\frac{3}{2}),$ $(011\frac{3}{2}0\frac{1}{2}), (211\frac{3}{2}0\frac{1}{2}),$ $(011\frac{3}{2}2\frac{3}{2}), (011\frac{3}{2}2\frac{5}{2}),$ $(211\frac{3}{2}2\frac{3}{2}), (211\frac{3}{2}2\frac{5}{2})$	$(000\frac{1}{2}2\frac{3}{2}), (011\frac{1}{2}0\frac{1}{2}),$ $(211\frac{1}{2}0\frac{1}{2}), (011\frac{1}{2}2\frac{3}{2}),$ $(011\frac{1}{2}2\frac{5}{2}), (211\frac{1}{2}2\frac{3}{2}),$ $(211\frac{1}{2}2\frac{5}{2})$	$(00012\frac{3}{2}), (01100\frac{1}{2}),$ $(21100\frac{1}{2}), (01102\frac{3}{2}),$ $(01102\frac{5}{2}), (21102\frac{3}{2}),$ $(21102\frac{5}{2})$	$(00012\frac{3}{2})$
2	$\frac{3}{2}$	$(000\frac{3}{2}2\frac{3}{2}), (011\frac{3}{2}0\frac{1}{2}),$ $(211\frac{3}{2}0\frac{1}{2}), (011\frac{3}{2}2\frac{3}{2}),$ $(011\frac{3}{2}2\frac{5}{2}), (211\frac{3}{2}2\frac{3}{2}),$ $(211\frac{3}{2}2\frac{5}{2})$		$(00012\frac{3}{2})$	

TABLE II.  $\Lambda d$  scattering lengths,  $A_{0,3/2}$  and  $A_{0,1/2}$  (in fm), and hypertriton binding energy,  $B_{0,1/2}$  (in MeV), for several hyperon-nucleon interactions characterized by  $\Lambda N$  scattering lengths  $a_{1/2,0}$  and  $a_{1/2,1}$  (in fm). We give in parentheses the results obtained in Ref. [4] including only three-body  $S$  wave configurations.

$a_{1/2,0}$	$a_{1/2,1}$	$A_{0,3/2}$	$A_{0,1/2}$	$B_{0,1/2}$
2.48	1.41	31.9 (66.3)	-16.0 (-20.0)	0.129 (0.089)
2.48	1.65	-72.8 (198.2)	-13.8 (-17.2)	0.178 (0.124)
2.48	1.72	-40.8 (-179.8)	-13.3 (-16.6)	0.192 (0.134)
2.48	1.79	-28.5 (-62.7)	-12.9 (-16.0)	0.207 (0.145)
2.48	1.87	-22.0 (-38.2)	-12.5 (-15.4)	0.223 (0.156)
2.48	1.95	-17.9 (-27.6)	-12.1 (-14.9)	0.239 (0.168)
2.31	1.65	-76.0 (198.2)	-17.1 (-22.4)	0.113 (0.070)
2.55	1.65	-73.6 (198.2)	-13.6 (-16.8)	0.185 (0.130)
2.74	1.65	-72.1 (198.2)	-12.0 (-14.4)	0.244 (0.182)

TABLE III. Hypertriton binding energy (in MeV) for several hyperon-nucleon interactions characterized by  $\Lambda N$  scattering lengths  $a_{1/2,0}$  and  $a_{1/2,1}$  (in fm) which are within the experimental error bars  $B_{0,1/2} = 0.130 \pm 0.050$  MeV.

	$a_{1/2,1} = 1.41$	$a_{1/2,1} = 1.46$	$a_{1/2,1} = 1.52$	$a_{1/2,1} = 1.58$
$a_{1/2,0} = 2.33$	0.080	0.087	0.096	0.106
$a_{1/2,0} = 2.39$	0.094	0.102	0.112	0.122
$a_{1/2,0} = 2.48$	0.129	0.140	0.152	0.164

TABLE IV.  $\Sigma d$  scattering lengths,  $A'_{1,3/2}$  and  $A'_{1,1/2}$  (in fm), and position of the quasibound state  $B'_{1,1/2}$  (in MeV) for several hyperon-nucleon interactions characterized by  $\Lambda N$  scattering lengths  $a_{1/2,0}$  and  $a_{1/2,1}$  (in fm). We give in parentheses the results obtained in Ref. [4] with only three-body  $S$  waves.

$a_{1/2,0}$	$a_{1/2,1}$	$A'_{1,3/2}$	$A'_{1,1/2}$	$B'_{1,1/2}$
2.48	1.41	$0.14 + i 0.24$ ( $0.20 + i 0.26$ )	$19.82 + i 16.94$ ( $19.28 + i 25.37$ )	$2.92 - i 2.17$
2.48	1.65	$0.28 + i 0.27$ ( $0.36 + i 0.29$ )	$12.08 + i 38.98$ ( $-1.55 + i 42.31$ )	$2.84 - i 2.14$
2.48	1.72	$0.32 + i 0.28$ ( $0.40 + i 0.30$ )	$2.92 + i 43.20$ ( $-10.47 + i 40.25$ )	$2.82 - i 2.11$
2.48	1.79	$0.36 + i 0.29$ ( $0.44 + i 0.31$ )	$-8.00 + i 42.58$ ( $-17.33 + i 35.01$ )	$2.79 - i 2.10$
2.48	1.87	$0.40 + i 0.30$ ( $0.49 + i 0.33$ )	$-16.90 + i 37.08$ ( $-21.16 + i 28.54$ )	$2.77 - i 2.09$
2.48	1.95	$0.45 + i 0.31$ ( $0.54 + i 0.34$ )	$-21.73 + i 29.48$ ( $-22.44 + i 22.44$ )	$2.75 - i 2.08$
2.31	1.65	$0.28 + i 0.27$ ( $0.36 + i 0.29$ )	$19.01 + i 23.21$ ( $14.95 + i 31.61$ )	$2.88 - i 2.14$
2.55	1.65	$0.28 + i 0.27$ ( $0.36 + i 0.29$ )	$-12.81 + i 43.49$ ( $-21.04 + i 33.19$ )	$2.79 - i 2.11$
2.74	1.65	$0.28 + i 0.27$ ( $0.36 + i 0.29$ )	$-26.01 + i 17.95$ ( $-23.29 + i 13.32$ )	$2.73 - i 2.09$

# FIGURES

FIG. 1. Inverse of the  $(I, J) = (0, 1/2)$  and  $(0, 3/2)$   $\Lambda d$  scattering lengths as a function of the  $\Lambda N$   $a_{1/2,1}$  scattering length.

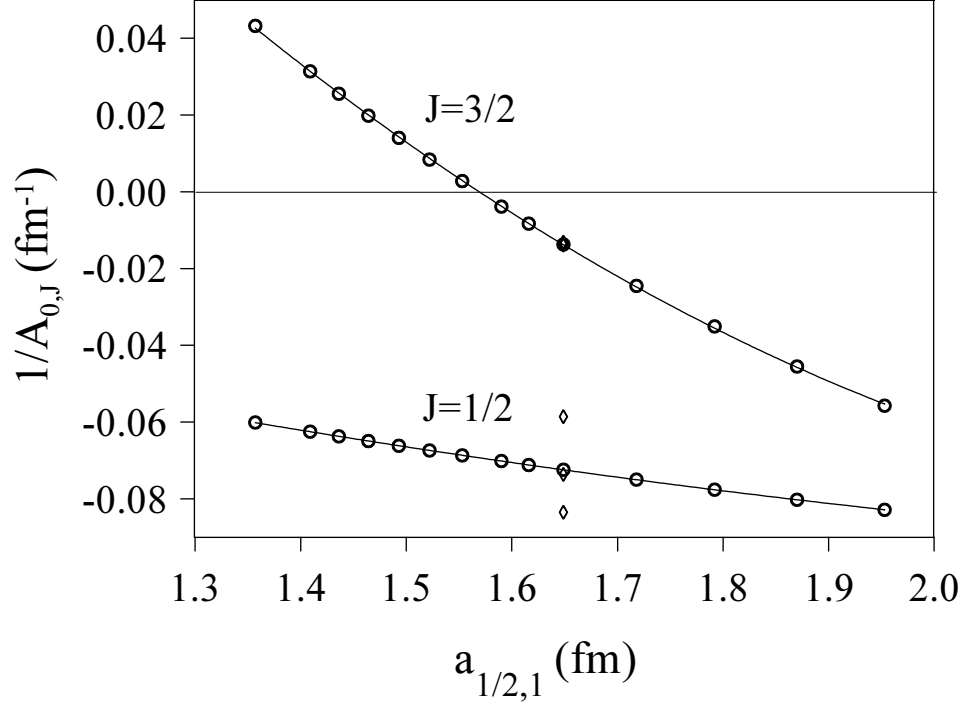


Figure 1

FIG. 2. Fredholm determinant for the  $\Lambda NN$  channels  $(I, J) = (1, 1/2)$  and  $(1, 3/2)$  for the model with  $a_{1/2,0} = 2.48$  fm and  $a_{1/2,1} = 1.41$  fm and energies below the  $\Lambda NN$  threshold.

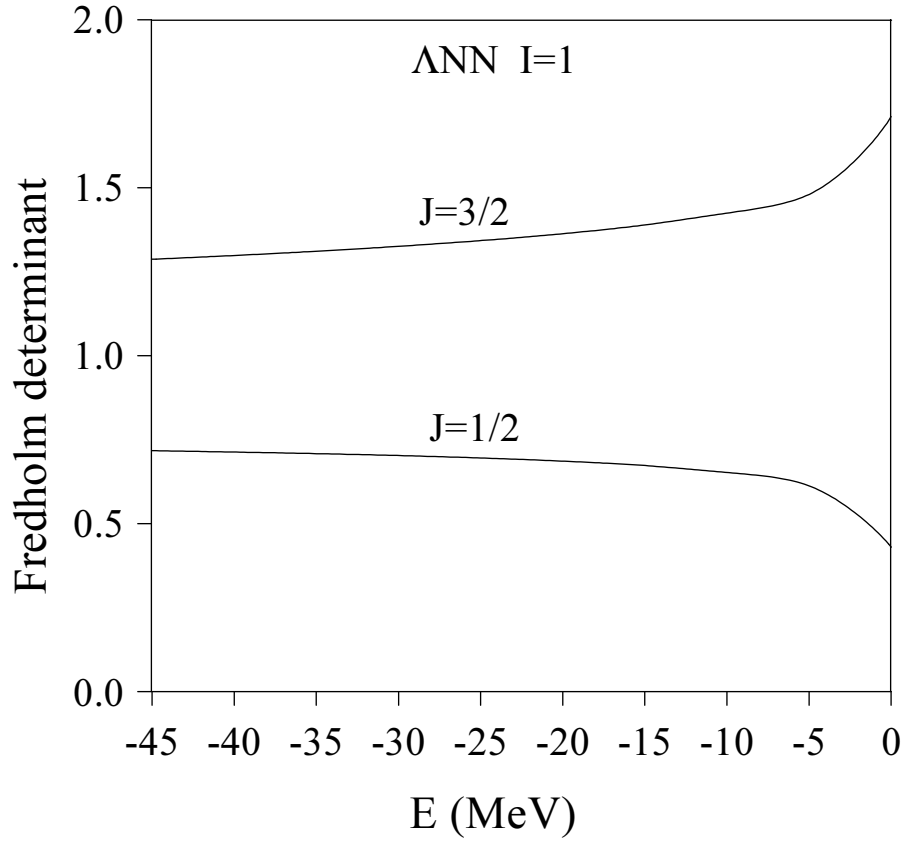


Figure 2

FIG. 3. Real and imaginary parts of the  $\Sigma d$  scattering length  $A'_{1,1/2}$  as a function of the  $\Lambda N$   $a_{1/2,1}$  scattering length.

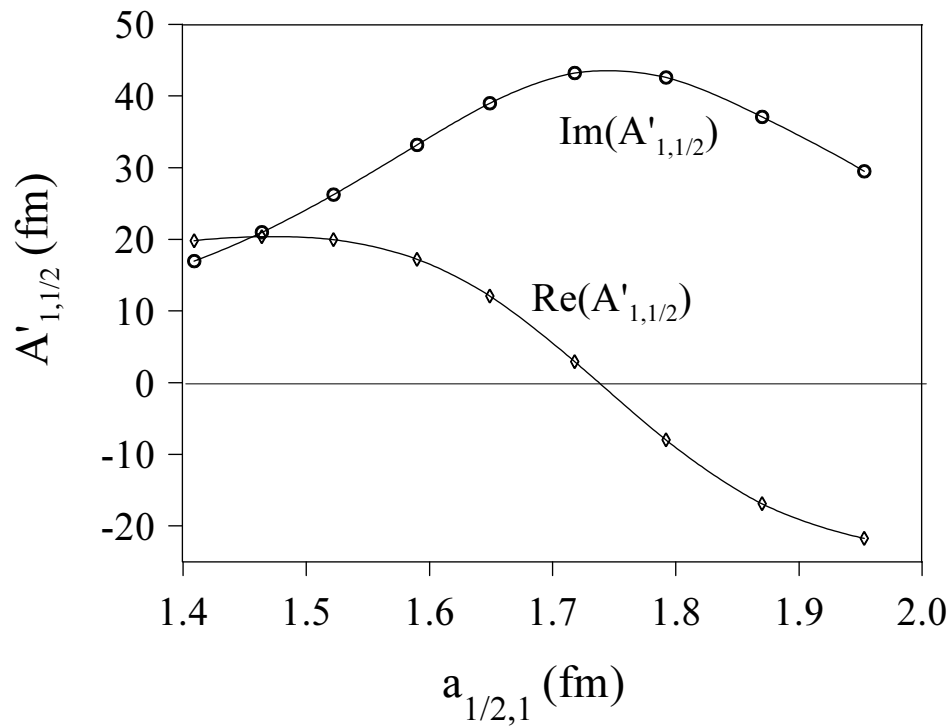


Figure 3



FIG. 4. Diagram that gives the most important contribution to the width of the  $\Sigma d$   $(I, J) = (1, 1/2)$  quasibound state.

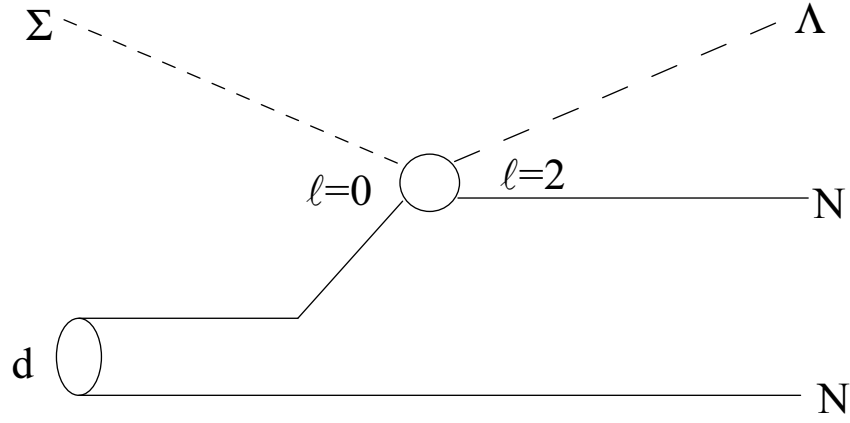


Figure 4

FIG. 5. Fredholm determinant for (a)  $J = 1/2$  and (b)  $J = 3/2$   $\Sigma NN$  channels for the model with  $a_{1/2,0} = 2.48$  fm and  $a_{1/2,1} = 1.41$  fm. The  $\Sigma d$  continuum starts at  $E = -2.225$  MeV, the deuteron binding energy obtained within our model.

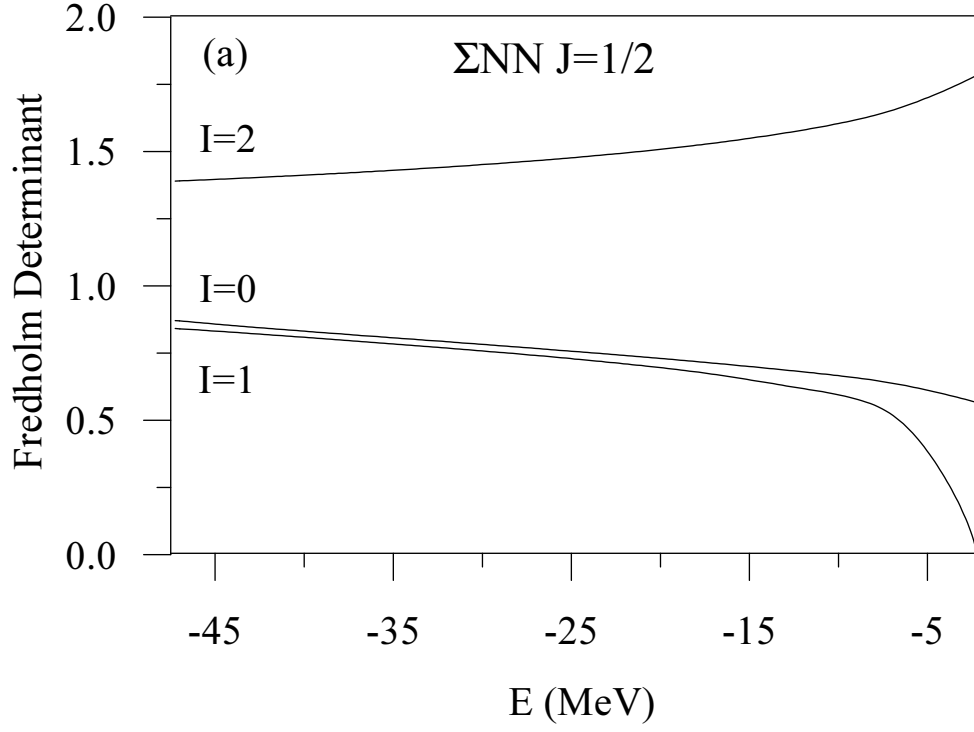


Figure 5

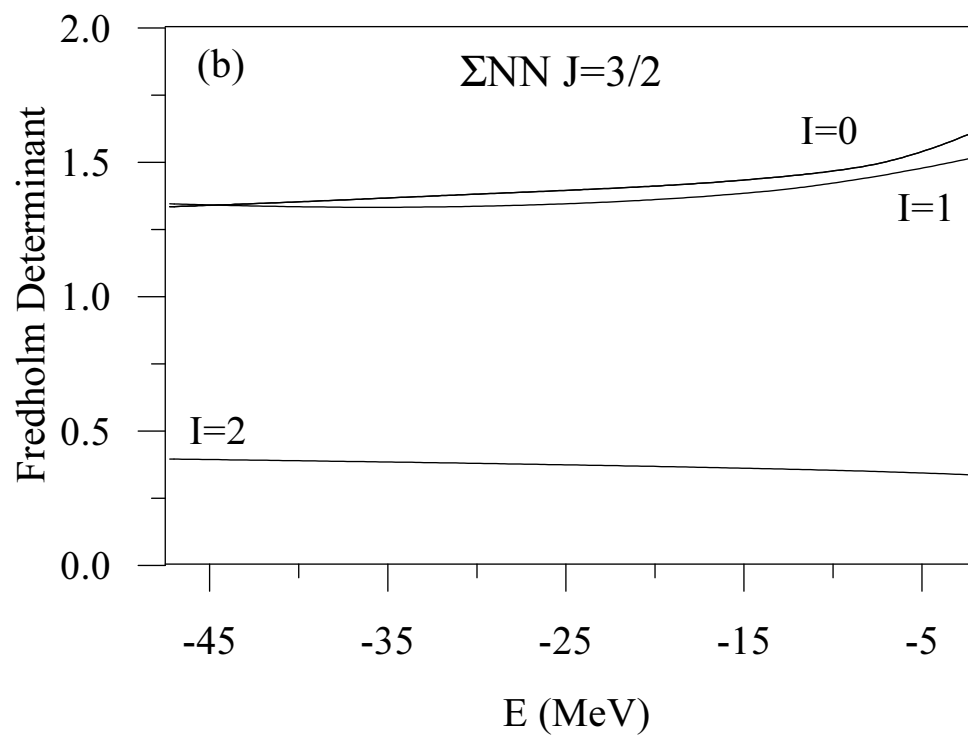


Figure 5